ACS OMEGA

Open Access

http://pubs.acs.org/journal/acsodf

Article

Copper Immobilized on Modified LDHs as a Novel Efficient Catalytic System for Three-Component Synthesis of Pyrano[2,3-*d*]pyrimidine and pyrazolo[4′,3′:5,6]pyrano[2,3-*d*]pyrimidine Derivatives

Sarieh Momeni and Ramin Ghorbani-Vaghei*

Cite This: *ACS Omega* 2024, 9, 10332−10342

Read Online

ACCESS | Metrics & More | Article Recommendations | Supporting Information

ABSTRACT: A novel catalyst based on layered double hydroxides coated with copper nitrate [LDH@(3-chloropropyl)trimethoxysilane@N1,N4-*bis*(4,6-diamino-1,3,5-triazin-2-yl)-benzene-1,4-disulfonamide@Cu] was successfully synthesized. The structure of the new synthesized catalyst was investigated and confirmed using different analytical techniques, such as Fourier-transform infrared spectroscopy (FTIR), energy-scattered X-ray spectroscopy (EDX) mapping, X-ray diffraction (XRD), field-emission scanning electron microscopy (FESEM), and heat gravity/heat derivatization (TGA/DSC). The skilled catalyst proved its efficiency for one-pot three-component synthesis of pyrano[2,3-*d*]pyrimidine and new dihydropyrazolo[4′,3′:5,6]pyrano[2,3-*d*]pyrimidine-dione derivatives. Using this efficient catalyst, products were synthesized with a high yield, in a short time, and under soft and solvent-free conditions. The catalyst can be recovered and reused four times without a significant loss of efficiency.

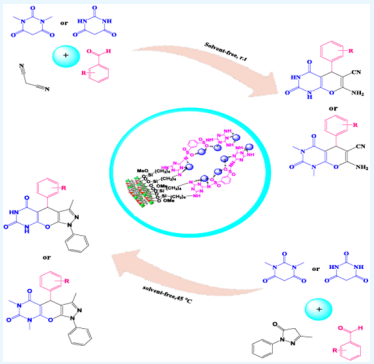

INTRODUCTION

Recently, much attention has been paid to layered double hydroxides (LDHs) due to their high active surface area, easy separation capability, and compound structure. LDHs can be used as an attractive base in various applications, such as medical, pharmaceutical, sensors, and drug delivery. As a result, they have attracted a lot of attention.[1−4] LDHs have a layered structure, which is also called hydrotalcite; it consists of divalent and trivalent cations, whose general formula is $[Me^{2+}(1-x)\ Me^{3+}\ x(OH)_2]^{x}+(An^{-})_{x/n}\ n\bullet H_2O$.[5,6] It is possible to change cations and anions, which may affect the properties of the layers. Today, layered double hydroxides are excellent supports for various catalysts due to the numerous hydroxide groups on their surface.[7−10]

Multicomponent reactions (MCRs) constitute one of the most important fields in organic synthesis, widely employed for their energy efficiency, high speed, ease, and cost-effectiveness.[11] In recent years, significant advances have been made in multicomponent reactions, with ongoing efforts focused on MCRs in the presence of new catalysts.[12−14] Pyrano[2,3-*d*]pyrimidines and their derivatives are heterocycle compounds containing nitrogen, utilized for their extraordinary medicinal and medical properties, including anticancer, antibacterial, antiviral, antihypertensive, antiallergic, anticoagulant, and antibronchitis effects.[15] Due to the myriad applications, the design of new catalysts for their synthesis is paramount. Synthesis of pyrano[2,3-*d*]pyrimidine derivatives, using different catalysts including Mn/ZrO_2,[16] cellulose-based nanocomposites,[17] nickel nanoparticles,[18] $Fe_3O_4@SiO_2@(CH_2)_3$-Urea-SO_3H/HCl,[19] Mn-ZIF-8@ZnTiO3,[20] sulfonic acid nanoporous silica (SBA-Pr-SO_3H),[21] $CoFe_2O_4$@Glutamin dysprosium,[22] SnO_2/SiO_2,[23] Fe_3O_4/Mo-MOF,[24] MgO nanopowders,[25] and nanobasic silica[11] has been explored.

Another important classification of heterocyclic compounds is pyrazolo-based pyranopyrimidines, known for their medicinal and pharmaceutical applications due to the fused three-ring structure comprising both pyranopyrazole and pyranopyrimidine patterns.[26,27] In 2014, in the presence of the DABCO catalyst (1,4-diazabicyclo[2.2.2]octane) pyrazolopyranopyrimidine derivatives were synthesized through a one-pot four-component reaction of ethyl acetoacetate, hydrazine hydrate, benzaldehyde derivatives, and barbituric acid in water under reflux conditions.[28] In 2018, using SBA-Pr-SO_3H, pyrazolopyranopyrimidine derivatives were synthesized through a condensation reaction of barbituric acids, aromatic aldehydes, and 3-methyl-5-pyrazolone.[29] Also, in two separate works in 2017, in the presence of an acid catalyst based on clay nanotubes and silica-supported ionic liquids, pyrazolopyranopyrimidine derivatives were synthesized via a domino reaction of ethyl acetoacetate, hydrazine hydrate, benzaldehyde derivatives, and barbituric acid.[30,31] Most of these methods are reported to have a long response time, low efficiency, and severe

Received: October 10, 2023
Revised: January 31, 2024
Accepted: February 9, 2024
Published: February 21, 2024

Scheme 1. Synthesis Route of LDH@TRMS@NDBD@Cu Nano-catalyst

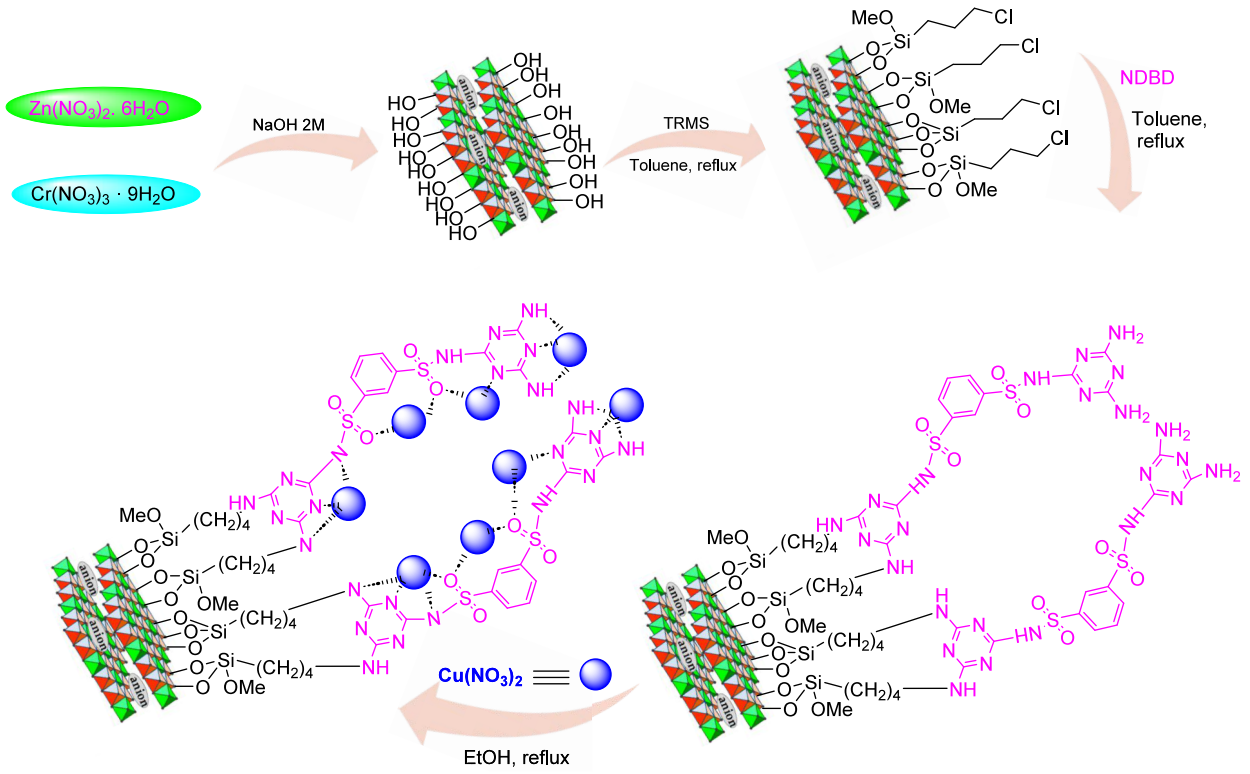

conditions. Finding a fast and environmentally friendly approach has thus attracted the attention of many researchers.

In this research, we have synthesized a novel LDH-based catalyst (LDH@(3-chloropropyl)trimethoxysilane@N1,N4-*bis*(4,6-diamino-1,3,5-triazin-2-yl)benzene-1,4-disulfonamide@Cu) and presented a simple, rapid, green, and high-efficiency method under mild conditions for the synthesis of pyrano[2,3-*d*]pyrimidine derivatives through a one-pot three-component condensation reaction. We used various benzaldehyde, malononitrile, and barbituric acid derivatives as raw materials. In a similar work, in the presence of this catalyst, new pyrazolo[4′,3′:5,6]pyrano[2,3-*d*]pyrimidine-dione derivatives were synthesized through a one-pot three-component reaction using raw materials, namely, 5-methyl-2-phenyl-2,4-dihydro-3H-pyrazole-3, benzaldehyde derivatives, and barbituric acid or 1,3-dimethylbarbituric acid.

EXPERIMENTAL

General. Solvents such as ethanol, methanol, ethyl acetate, normal hexane, toluene, and acetonitrile were prepared and purchased from Sigma-Aldrich Company. Used chemicals in the study include $Zn(NO_3)_2{\cdot}6H_2O$, $Cr(NO_3)_3{\cdot}9H_2O$ salts, 1,3-Benzenedisulfonic acid disodium salt, melamine, copper nitrate, malononitrile, benzaldehyde derivatives (e.g., 4-nitro, 3-nitro, 4-fluoro, 4-methyl, 4-methoxy, 4-hydroxy, 3-hydroxy, 4-chloro, 2-chloro, 2,4-dichloro, 4-bromo, and 4-dimethylamino benzaldehyde), barbituric acid, 1,3-dimethylbarbituric acid, and 5-methyl-2-phenyl-2,4-dihydro-3H-pyrazol-3-one, which were obtained from Merck Company. Additionally, 3-chloropropyltrimethoxysilane, benzaldehyde, and PCl_5 were prepared and purchased from Sigma-Aldrich Company. The melting points of the samples were determined using the Electrothermal 9200 device and have not been modified. ^1H and ^{13}CNMR spectra of the products were taken using the Varian INOVA 500 MHz device. The FTIR spectrum of the samples was obtained using KBr tablets and the PerkinElmer GX FTIR device. EDX analysis was conducted using Bruker EDAX-EDS device. Thermal gravimetric analysis using a TGA STA6000 device was recorded. TGA and DSC analyses of the sample were conducted under a nitrogen atmosphere at a rate of 10 °C per minute, ranging from ambient temperature to 560 °C. X-ray diffraction (XRD) was performed using a Philips PW1730 XRD device. Field-emission scanning electron microscopy (FESEM) images were recorded by FESEM ZEISS Sigma 300 and FESEM MIRA3 TESCAN device covered with a gold foil.

Synthesis of Hydrotalcites. LDH containing nickel and chromium metals was synthesized through the coprecipitation of $Zn(NO_3)_2.6H_2O$ and $Cr(NO_3)_3.9H_2O$ salts in a molar ratio of 2:1 in deionized water. The pH of the solution was raised to 11.5 using a 2 M soda solution, and it was maintained at a temperature of 65 °C for 18 h. Subsequently, the turquoise slurry was filtered using filter paper, washed several times with distilled water, and dried in an oven at a temperature of 60 °C.[32]

Synthesis of LDH@TRMS. To functionalize LDHs with chlorine, we used 3-chloropropyltrimethoxysilane (TRMS) and 1 g of synthesized LDHs from the previous step was mixed with 1 mL of TRMS in 50 mL of toluene and placed under reflux conditions for 24 h. The resulting mixture was then filtered and washed several times with toluene and once with distilled water (2 mL). Finally, it was placed in an oven at a temperature of 60 °C to dry for 18 h.

Procedure for Synthesis of 1,3-Benzenedisulfonyl Chloride. 1,3-Benzenedisulfonic acid disodium salt was added to the chlorine agent (PCl_5) in a flask and stirred for 2 h at 65 °C, then some ice was added to the reaction vessel and the product was isolated with chloroform (100 mL).

https://doi.org/10.1021/acsomega.3c07913
ACS Omega 2024, 9, 10332−10342

Procedure for Synthesis of Ligand: N1,N4-Bis(4,6-diamino-1,3,5-triazin-2-yl)benzene-1,4-disulfonamide (NDBD). In a 50 mL round-bottom flask, 1,3-benzenedisulfonyl chloride (2 mmol) was dissolved in toluene solvent (30 mL), and in another container melamine (4 mmol) was dissolved in toluene, then the container containing melamine mixture was added dropwise to the flask. Subsequently, the vessel was placed under reflux conditions for 24 h. Afterward, the precipitate was filtered and washed several times with acetonitrile (3 mL). Finally, the product was placed to dry at 60 °C for 18 h.

Procedure for Synthesis of LDH@TRMS@NDBD. In a 250 mL round-bottom flask, 0.3 g of LDH@TRMS was added, and 50 mL of toluene was used as the solvent. The mixture was placed in an ultrasonic device for 30 min. Then, ligand N1,N4-*bis*(4,6-diamino-1,3,5-triazin-2-yl)benzene-1,4-disulfonamide was added, and the solution was stirred for 48 h under reflux conditions. Afterward, the resulting combination was filtered and washed several times with toluene (2 mL) and once with ethanol (2 mL). Finally, the product was placed in an oven at a temperature of 60 °C for 24 h.

Procedure for Synthesis of LDH@TRMS@NDBD@Cu(NO_3)$_2$. The mixture obtained from the previous step (0.5 g) was added to a 25 mL flask containing 10 mL of ethanol. Then, the mixture was dispersed in an ultrasonic device for 15 min, and copper nitrate (0.23 g) was added. The resulting solution was placed under reflux conditions for 24 h. The obtained product was separated by centrifugation, washed several times with ethanol (2 mL), and placed in the oven at a temperature of 60 °C for 24 h (Scheme 1).

Procedure for the Synthesis of Pyrano[2,3-*d*]-pyrimidine Derivatives in the Presence of the LDH@TRMS@NDBD@Cu(ii) Catalyst. In a test tube, malononitrile (1 mmol), benzaldehyde derivatives (1 mmol), and barbituric acid or 1,3-dimethylbarbituric acid (1 mmol), along with the LDH@TRMS@NDBD@Cu(II) catalyst (0.045 g) were stirred for a suitable period of time at room temperature. The progress of the reaction was checked by TLC (*n*-hexane: ethyl acetate; 5:5). After the completion of the reaction, the catalyst was separated by adding hot ethanol (2 mL), centrifuged, and washed with ethanol (2 mL). The pure products were obtained by recrystallization with ethanol.

General Procedure for the Synthesis of Pyrazolo-[4,3:5,6]pyrano[2,3-*d*]pyrimidine-dione Derivatives in the Presence of LDH@TRMS@NDBD@Cu NPs. In a test tube, 5-methyl-2-phenyl-2,4-dihydro-3H-pyrazol-3-one (1 mmol), benzaldehyde derivatives (1 mmol), and barbituric acid or 1,3-dimethylbarbituric acid (1 mmol) along with the LDH@TRMS@NDBD@Cu(II) catalyst (0.045 g), were stirred for a suitable period of time at a temperature of 45 °C. The progress of the reaction was checked by TLC (*n*-hexane: ethyl acetate; 5:5). After the completion of the reaction, the catalyst was separated by adding hot ethanol, centrifuged, and washed with ethanol (2 mL). The pure products were obtained by recrystallization with ethanol.

RESULTS AND DISCUSSION

Catalyst Characterization. Figure 1 shows the FTIR spectra of LDHs (a), LDH@TRMS (b), melamine (c), NDBD (d), LDH@TRMS@NDBD (e), and LDH@TRMS@NDBD@Cu (f). According to Figure 1, the broad peak at 3508 cm^{-1} is related to the hydroxyl groups of LDH, which is clearly visible in part (a), and also in part (b). In addition to this, the peak at 2951 cm^{-1} is related to CH stretching vibrations, and the peak observed in the region of 1100 cm^{-1} is associated with the C−H propyl vibrations, indicating the placement of 3-chloropropyltrimethoxysilane on the layered double hydroxide. In part (c) of the spectrum, related to melamine, peaks related to NH are observed in the region 3133−3470 cm^{-1}, and the stretching vibrations of ring cyanide are shown in the region 1652 and 1631 cm^{-1}. In part (d), related to the ligand of NDBD, the peaks in the 3200−3400 cm^{-1} region are related to the stretching vibrations of NH on the ligand. Peak 1722 cm^{-1} is related to the stretching vibrations of ring cyanide, which has shifted from 1652 cm^{-1} to this region due to the formation of the sulfonyl amide group in the vicinity of ring cyanide. Also, peak 1679 cm^{-1} is related to ring cyanide, shifted from region 1631 to 1679 cm^{-1}, and the peaks at 1360 and 1143 cm^{-1} correspond to SO stretching vibrations. In part (e), the hydroxyl peaks were covered, and the ligand was placed on it. Vibrations related to NH (3100−3400 cm^{-1}) and SO (1358 and 1143 cm^{-1}) are observed, and the peak in the region 2957 cm^{-1} corresponds to the CH stretching vibrations of the 3-chlorotrimethoxysilane group, confirming the complete linking of the ligand to LDHs. In the last stage (f), it can be seen that stretching vibrations to NH and SO groups have decreased sharply. Also, the peaks of 517, 574, and 1384 cm^{-1} are related to copper nitrate, indicating successful placement of copper nitrate on the catalyst. The ^{1}HNMR and ^{13}CNMR spectra of ligand N1,N4-bis(4,6-diamino-1,3,5-triazin-2-yl)benzene-1,4-disulfonamide (NDBD) are shown in Figure 2. Part (a) corresponds to the ^{1}HNMR of NDBD in DMSO solvent. The peak appearing at δ 12.28 with integral 2 is related to two NHs connected to the SO_2 group, and a peak at δ 7.82 with an integral of 8 corresponds to the NH_2 group of the ligand. The two-branch peak at δ 7.55−7.58 with an integral of 2 is related to two protons on the benzene ring in the vicinity of the carbon attached to the SO_2 group. The single protons of the benzene ring with an integral of 1 appear at δ 7.27−7.33 and δ 8.39, respectively, as a tribrach and a monobranch. Part (b) is the ^{13}C NMR spectrum of the NDBD ligand. The peak at δ 147.4 is related to two carbons of the benzene ring connected to the SO_2 group. The rest of the carbons of the benzene ring that are not directly connected to SO_2 appear at δ 123−128, and the peak at δ 159.9 is related to the carbon connected to the NH_2

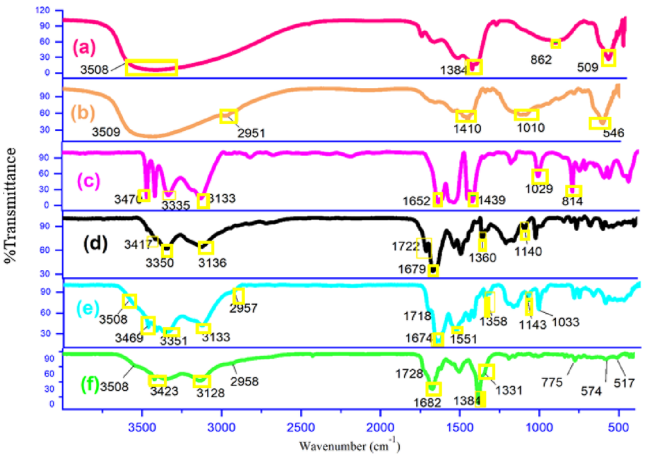

Figure 1. FTIR spectra of (a) LDHs, (b) LDH@TRMS, (c) melamine, (d) ligand of NDBD, (e) LDH@TRMS@NDBD, and (f) LDH@TRMS@NDBD@Cu.

https://doi.org/10.1021/acsomega.3c07913
ACS Omega 2024, 9, 10332−10342

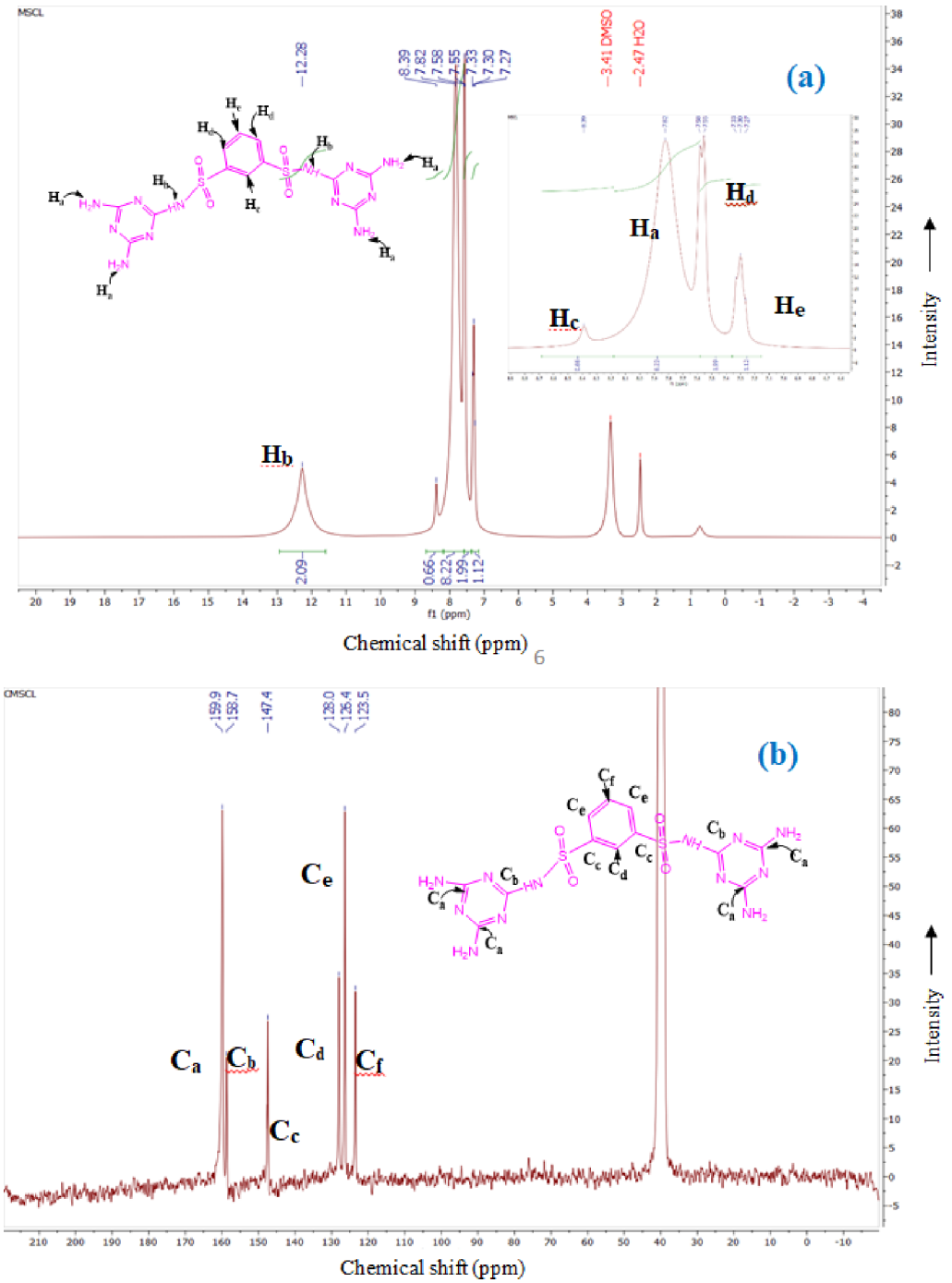

Figure 2. ^{1}H NMR (250 MHz) (a) and ^{13}CNMR (63 MHz) (b) spectrum of the NDBD ligand.

group. The peak at δ 147.4 corresponds to the carbon attached to the NH group.

Also, in another study, elemental determination analysis by energy-dispersive spectrometer was conducted on the constituent elements of the LDH@TRMS@NDBD@Cu nanocatalyst. The results of this test confirmed the presence of oxygen, nitrogen, carbon, sulfur, silicon, copper, zinc, and chromium elements in the catalyst structure (Figure 3). Additionally, according to Figure 4, elemental analysis of the composition confirms the synthesis of the LDH@TRMS@NDBD@Cu catalyst and the presence of the mentioned elements.

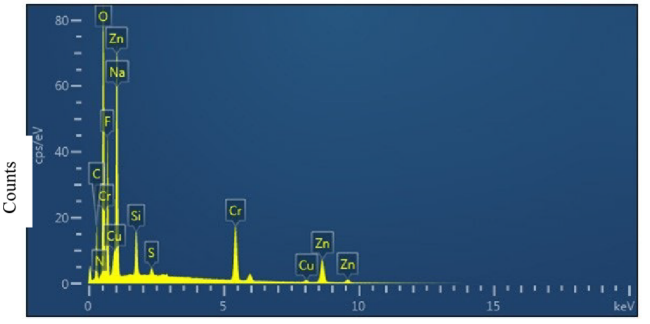

Figure 3. EDX spectra of LDH@TRMS@NDBD@Cu.

https://doi.org/10.1021/acsomega.3c07913
ACS Omega 2024, 9, 10332−10342

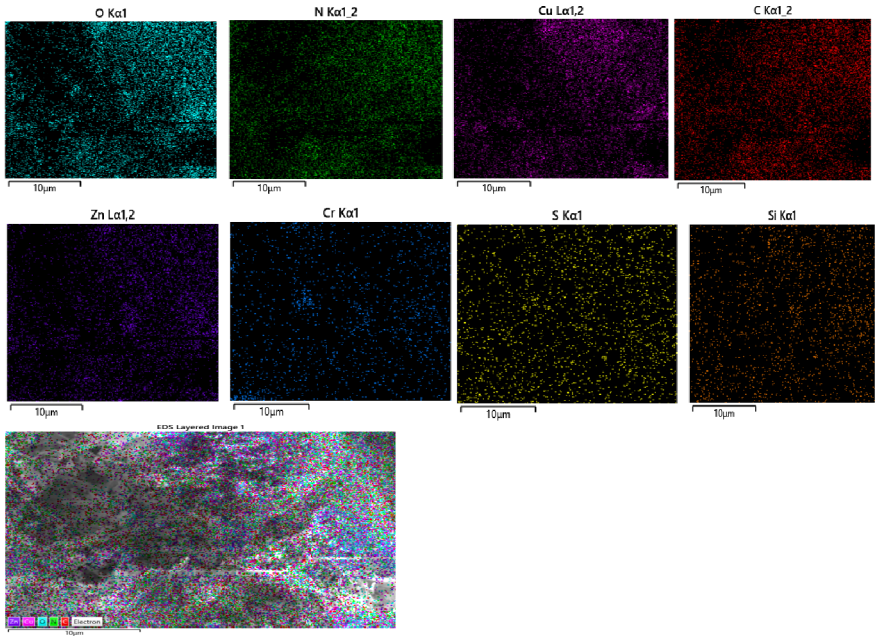

Figure 4. Elemental mapping of Cr (blue), Zn (dark purple), N (green), O (turquoise), C (red), Cu (bright purple), and Si (orange) atoms for LDH@TRMS@NDBD@Cu.

In order to investigate the structure, morphology, and size of particles, the images related to the FESEM of LDH@TRMS@NDBD@Cu are shown in Figure 5. As is evident from the image (part (a)), it depicts the basic form of LDHs with a hexagonal and flat layer structure (part (a)), measuring approximately 5 μm in size. By placing the ligand and copper nitrate metal on it, the surface of the catalyst is roughened, and nanoparticles with a spherical and uniform morphology can be seen on it (part (b)). Pictures (b_1) and (b_2) are of the LDH@TRMS@NDBD@Cu catalyst taken by FESEM ZISS device, where the size of the nanoparticles is not clearly visible. Images (b_3) and (b_4) are of the LDH@TRMS@NDBD@Cu catalyst taken with the FESEM MIRA3 TESCAN device, which clearly illustrates the hexagonal structure of the LDH layer, proving that the LDH layer's structure is preserved after placing the ligand and copper nitrate metal (image (b_3)). However, the surface is uneven, and nanoparticles can be observed on it, and shows the size of the nanoparticles ranging from 18 to 28 nm (image (b_4)).

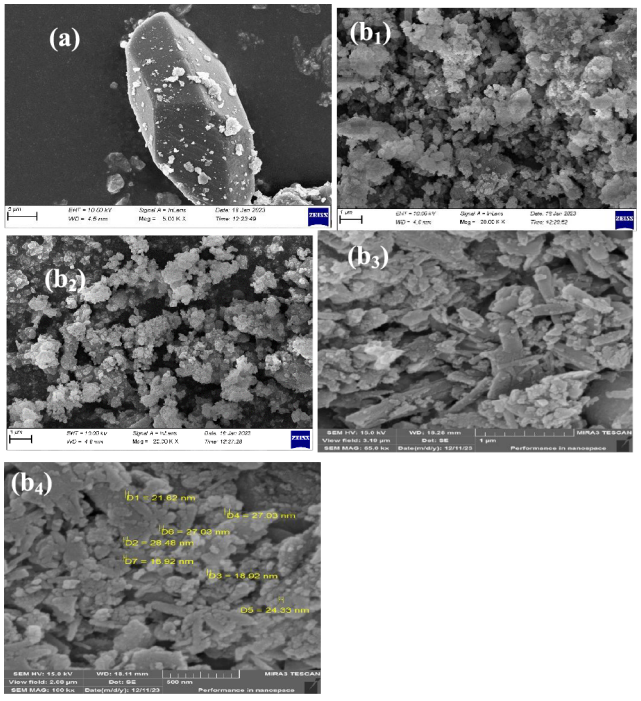

Figure 5. FESEM images of LDHs (a), LDH@TRMS@NDBD@Cu (b_1, b_2, b_3, b_4).

XRD spectrum related to the stages of catalyst synthesis has been performed in the 2θ region

from 10° to 80°. XRD patterns of LDHs, LDH@TRMS, and LDH@TRMS@NDBD@Cu can be seen in Figure 6. According to Figure 6a,b,[31] the intensity and position of all the peaks appearing at 11°, 24°, 33°, 35°, 37°, 48°, 52°, 60°, and 68° correspond to the standard pattern of zinc/chromium layered double hydroxides. As evident in Figure 6c, the peaks appearing at 14.95°, 21.12°, 29.25°, 31.78°, 33.31°, 36.26°,

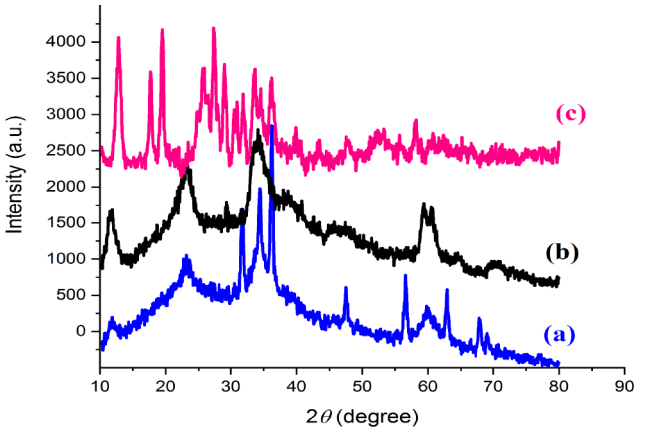

Figure 6. XRD pattern of (a) LDHs, (b) LDH@TRMS, and (c) LDH@TRMS@NDBD@Cu nanocomposites.

https://doi.org/10.1021/acsomega.3c07913
ACS Omega 2024, 9, 10332−10342

39°, 41°, 43.41°, 49°, 51.25°, 53.35°, and 57.98°, in accordance with the standard pattern of copper nitrate,[33] confirm that copper nitrate metal is successfully placed on the catalyst, showing the final structure of the catalyst with high crystallinity. The particle size was found to be approximately 10 nm using Scherrer's equation.

To assess the thermal stability of catalyst 1, weight-thermal analysis (TGA) was performed. According to Figure 7, the

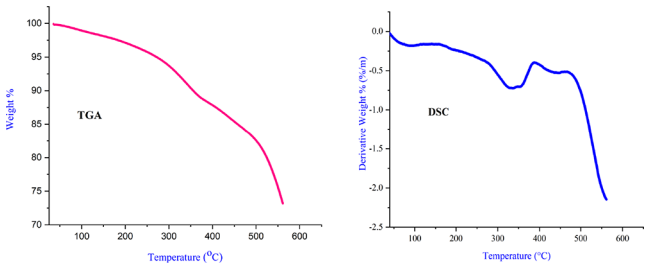

Figure 7. TGA and DSC curves of LDH@TRMS@NDBD@Cu between 30 and 760 °C.

initial weight loss occurs in the range of 100−170 °C, possibly attributed to the presence of water and solvents used in the catalyst synthesis. Subsequently, a subsequent weight loss at a higher temperature (range of 200−270 °C) is observed, attributed to the loss of interlayer anions and the solvents trapped within these layers. The third weight loss, occurring between 330 and 520 °C, is ascribed to the destruction and separation of the ligand attached to LDHs. Beyond 520 °C, it results in the removal of the metal and the breakdown of the catalyst. All the breakdown areas observed in the TGA analysis align with the changes noted in the DSC analysis. Similar to TGA, in the DSC analysis, the range from 100 to 170 °C represents the endothermic region, leading to the elimination of solvents and trapped water. The interval from 370 to 520 °C corresponds to the removal of the ligand, and above 520 °C, it results in the decomposition of the catalyst and the removal of copper nitrate from the catalyst surface. The DSC analysis confirms the TGA analysis and shows the stability of the catalyst up to 370 °C. Considering the stability of the catalyst in a very high temperature range, this can be attributed to the strong interaction between the ligand and LDHs, coupled with its complexation with copper nitrate. This strong interaction effectively prevents catalyst decomposition at lower temperatures.

CATALYTIC STUDIES

Optimization of Main Effective Parameters for Pyrano[2,3-*d*]pyrimidine Synthesis. To optimize the reaction conditions and check the efficiency of the catalyst, factors such as temperature, different amounts of the catalyst, various solvents, and reaction time were carefully investigated (Table 1). For this purpose, malononitrile, 4-chlorobenzaldehyde, and 1,3-dimethylbarbituric acid were used as a model reaction under different conditions. The model test was also conducted in the absence of the catalyst, resulting in a small yield of the product. The best conditions were achieved at room temperature with 0.045 g of the catalyst. A noteworthy point is that the reaction is conducted without a solvent at room temperature, highlighting the green nature of the protocol. Copper on the catalyst interacts well with the raw materials, leading to a high yield of products in a short time

Table 1. Optimization of Pyrano [2,3-*d*]-pyrimidine Synthesis in the Presence of LDH@TRMS@NDBD@Cu Catalyst[a]

entry	catalyst (mg)	solvent	temperature (°C)	time (min)	yield (%)[b]
1b			r.t.	60	12
2	10		r.t.	15	67
3	20		r.t.	15	73
4	35		r.t.	10	86
5	45		r.t.	3	97
6	50		r.t.	5	97
7	45		70	3	95
8	45	EtOH	reflux	15	70
9	45	MeOH	reflux	25	68
10	45	EtOH/H_2O	reflux	25	91
11	45	CH_3CN	reflux	15	85
12	45	H_2O	reflux	15	86

[a]Reaction conditions: 4-chlorobenzaldehyde (1 mmol), malononitrile (1 mmol), barbituric acid, or 1,3-dimethylbarbituric acid (1 mmol). [b]Isolated yield.

Table 2. Comparison of the Catalytic Activity of GO@Fe_3O_4@TRMS@HBPB@Cu Catalyst and its Related Intermediates[a]

entry	catalyst	time	yield (%)[b]
1	LDHs	30	38
2	LDH@TRMS	30	20
3	LDH@TRMS@NDBD	20	88
4	LDH@TRMS@NDBD@Cu$(NO_3)_2$	5	95

[a]Reaction conditions: 4-chlorobenzaldehyde (1 mmol), malononitrile (1 mmol), barbituric acid, or 1,3-dimethylbarbituric acid (1 mmol). [b]Isolated yield.

and without the need for a solvent. If a smaller amount of the LDH@TRMS@NDBD@Cu catalyst is used, then the efficiency decreases, indicating the high performance of the catalyst. As evident from Table 1, the model reaction was performed in the presence of methanol, ethanol, water, ethyl acetate, and water/ethanol solvents, resulting in good yields. The water and ethanol solvent showed a higher yield than the others. However, in the absence of a solvent, the highest efficiency was observed, and the yield of the reaction was negligible without the catalyst. The model reaction was also investigated in the presence of catalyzed intermediates, as compiled in Table 2. LDHs produced 38% of the product in half an hour. With the addition of 3-chlorotrimethoxysilane on the surface of LDHs, the yield of the product decreased. However, when the ligand was applied to the surface of LDH@TRMS, the yield of the product increased dramatically, and the reaction time was reduced to 20 min. The highest yield of the product was obtained in 5 min in the presence of copper nitrate stabilized on the surface of LDH@TRMS@NDBD, demonstrating the high efficiency of the catalyst.

Investigating the Catalytic Activity in the Three-Component One-Pot Synthesis of Pyrano[2,3-*d*]-pyrimidine and Dihydropyrazolo[4′,3′:5,6]pyrano[2,3-*d*]pyrimidine-dione Derivatives. To investigate the performance of the new LDH@TRMS@NDBD@Cu catalyst, the synthesis of pyrano[2,3-*d*]pyrimidine derivatives was conducted under optimal conditions using malononitrile, barbituric acid or 1,3-dimethylbarbituric acid along with a wide range of benzaldehydes with different donor and acceptor

https://doi.org/10.1021/acsomega.3c07913
ACS Omega 2024, 9, 10332−10342

Table 3. Synthesis of Pyrano[2,3-*d*]pyrimidine and Dihydropyrazolo[4′,3′:5,6]pyrano[2,3-*d*]pyrimidine-dione Derivatives in the Presence of LDH@TRMS@NDBD@Cu Nanocatalyst[a]

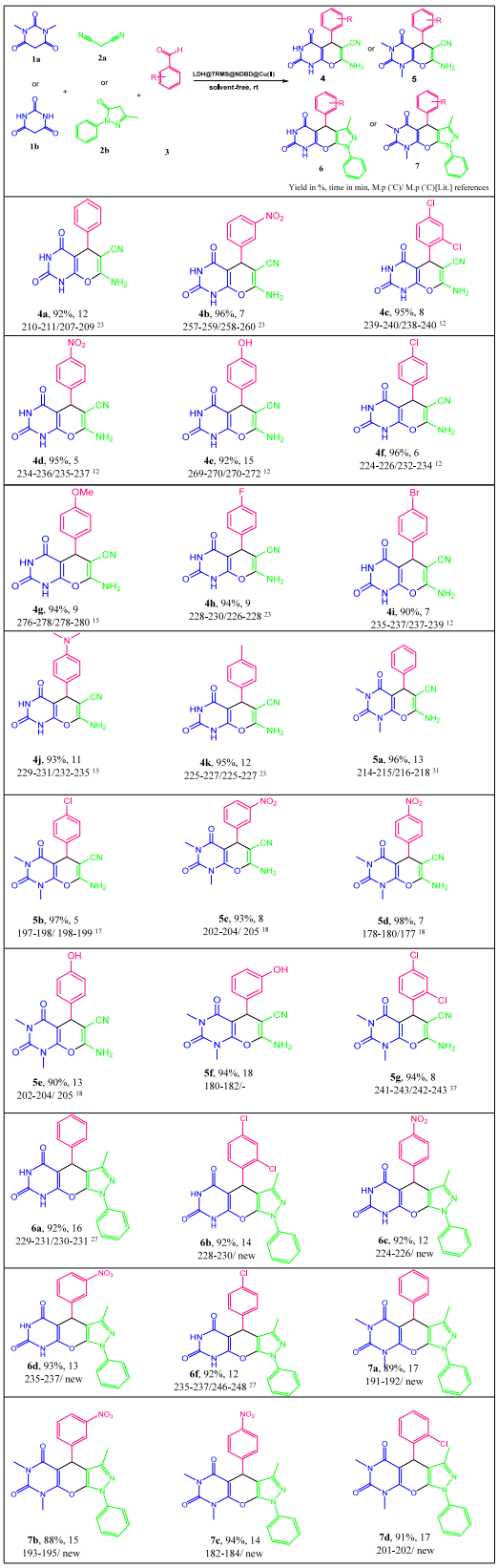

[a]Isolated yield.

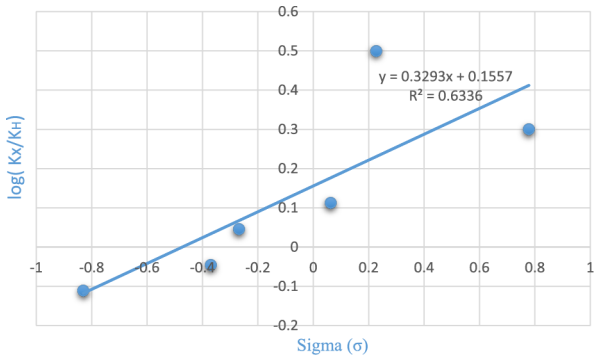

Figure 8. Hammett plot for investigation of the substitution groups in the synthesis of pyrano[2,3-*d*]pyrimidine.

groups. The reaction proceeded rapidly, resulting in high product yields (Table 3). Some products with electron-donating aldehydes required a slightly higher temperature. Benzaldehydes with electron-withdrawing groups in the ortho and para positions produce the product in higher yields and shorter reaction times. This is because carbonyl benzaldehydes with electron-withdrawing groups become more positive and sensitive, reacting more easily with malononitrile in the presence of a catalyst. A Hammett diagram was employed to investigate the effect of different substitutions of benzaldehyde in the synthesis reaction of pyrano[2,3-*d*]pyrimidine (Figure 8). The slope of the graph (ρ: 0.3293) indicates that the reaction to electron-killing substitutions is more sensitive than to electron-donating substitutions. The positive value ρ indicates that the reaction rate increases with electron-killing substitutions, suggesting the negativity of the transition state stabilized by electron-killing substitutions on benzaldehyde. In another part of investigating the efficiency of the catalyst, dihydropyrazolo[4′,3′:5,6]pyrano[2,3-*d*]pyrimidine-dione derivatives were synthesized in the presence of the new LDH@TRMS@NDBD@Cu catalyst under three-component one-pot conditions. These derivatives were synthesized for the first time using three components of raw materials: barbituric acid or 1,3-dimethylbarbituric acid, 5-methyl-2-phenyl-2,4-dihydro-3*H*-pyrazol-3-one, and a wide range of benzaldehydes with different donor and acceptor groups. The results demonstrated the high efficiency of the catalyst in the synthesis of these compounds, achieving high yields and short reaction times. The synthesized dihydropyrazolo[4′,3′:5,6]pyrano[2,3-*d*]-pyrimidine-dione derivatives are listed in Table 3.

Mechanistic Evaluation. The proposed mechanism for the synthesis of pyrano[2,3-*d*]pyrimidine regarding the catalytic role is illustrated in Scheme 2. As evident from the scheme, the interaction between chelated copper and the carbonyl group of benzaldehyde and malononitrile creates intermediate A. Intermediate A reacts with barbituric acid or 1,3-dimethylbarbituric acid, whose carbonyl group interacts with the copper catalyst, forming intermediate B. Through tautomerism, which occurs in the presence of chelated copper, the final product is synthesized, and the catalyst is recovered for use in subsequent reactions. According to the mechanism, it is evident that the carbonyl groups of benzaldehyde and barbituric acid, as well as the nitrogen in malononitrile, play a key role in this reaction by interacting with copper supported on the catalyst, contributing to improved reaction conditions and facilitating the synthesis process. The synthesis mechanism of dihydropyrazolo[4′,3′:5,6]pyrano[2,3-*d*]pyrimidine-dione

https://doi.org/10.1021/acsomega.3c07913
ACS Omega 2024, 9, 10332−10342

Scheme 2. Suggested Mechanism for the Synthesis of Pyrano[2,3-*d*]pyrimidine with the Catalytic Role of LDH@TRMS@NDBD@Cu

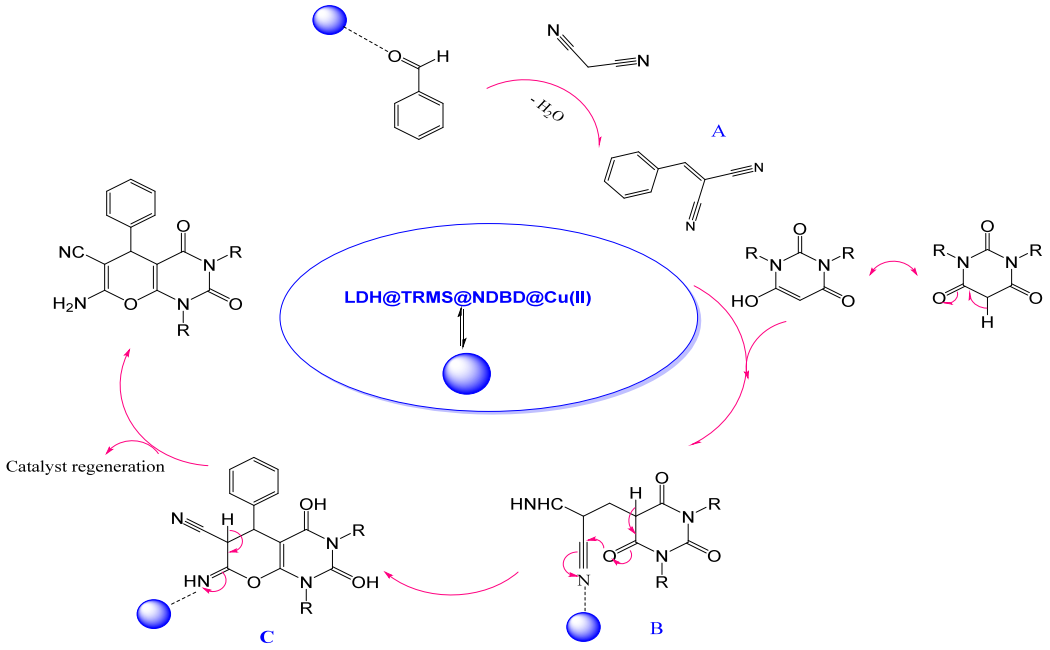

Scheme 3. Suggested Mechanism for the Synthesis of Dihydropyrazolo[4′,3′:5,6]pyrano[2,3-*d*]pyrimidine-dione with the Catalytic Role of LDH@TRMS@NDBD@Cu

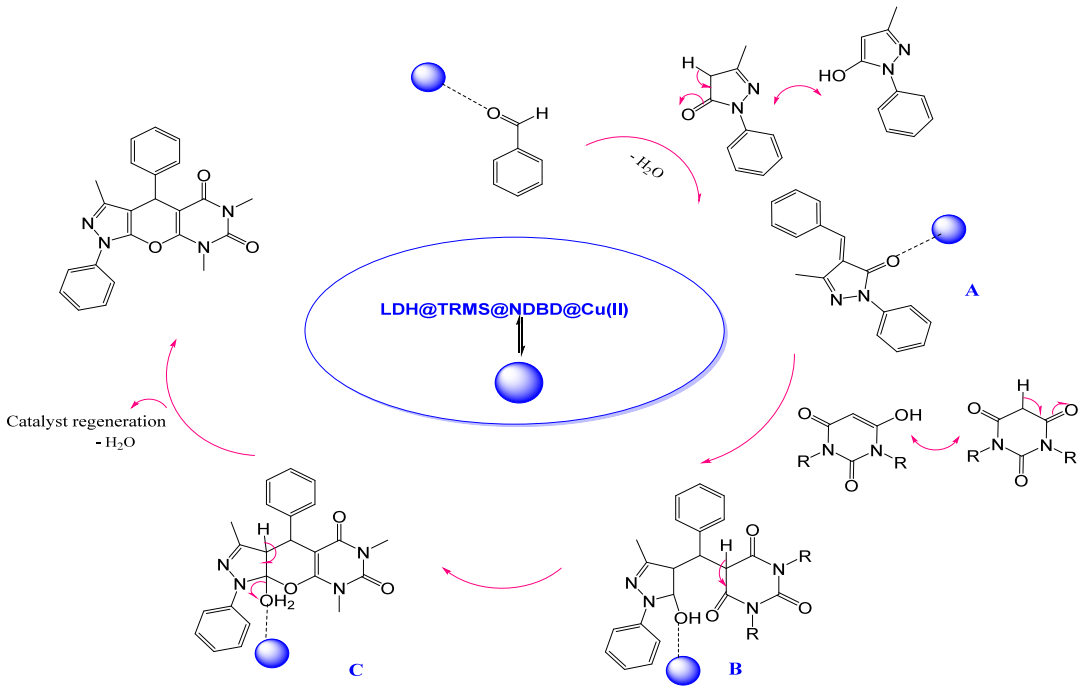

derivatives using the LDH@TRMS@NDBD@Cu catalyst is depicted in Scheme 3, which shares almost the same synthesis mechanism as pyranopyrimidines. According to Scheme 3, the initial interaction of the copper chelate of the catalyst with the carbonyl aldehyde group induces the positive charge on the oxygen of the carbonyl aldehyde group, making it susceptible to attack by 5-methyl-2-phenyl-2,4-dihydro-3*H*-pyrazol-3-one, resulting in the formation of intermediate A. Subsequently, intermediate B is formed from the reaction of barbituric acid or 1,3-dimethylbarbituric acid with intermediate A in the presence of the copper chelate catalyst. Continuing the reaction, intermediate C is created through internal oxygen attack. In the final step, the product is synthesized by removing the water molecule, and the catalyst is recycled, returning to the reaction cycle.

Reusability Study of Catalyst. Investigating the reusability of the catalyst, which is biologically and economically important, an analysis was carried out for the newly synthesized catalyst. After the synthesis of the products, hot ethanol was added to the reaction container to extract the

https://doi.org/10.1021/acsomega.3c07913
ACS Omega 2024, 9, 10332−10342

Table 4. Comparison of LDH@TRMS@NDBD@Cu Catalyst Activity in Pyranopyrimidine Synthesis with Several Catalysts

entry	reaction conditions	time (min)	yield (%)	lit.
1	Mn/ZrO_2, EtOH: H_2O, r.t.	60	90	16
2	TMU-16-NH_2, H_2O, reflux	60	97	34
3	Fe_3O_4/Mo-MOF core−shell, H_2O: EtOH (1:1), 40 °C	25	93	24
4	SnO_2/SiO_2, EtOH	60	94	23
5	urea, neat, 140 °C	840	86	21
6	SBA-Pr-SO_3H, neat, 140 °C	15	90	35
7	PC/AgNPs, EtOH: H_2O, reflux	10	94	36
8	Zn[(l)proline]$_2$, EtOH/reflux	0.5−12 h	90	37
9	(SiO_2@Glu/Si $(OEt)_2(CH2)_3N$ = Mo $[Mo_5O_{18}]$, solvent-free, 80 °C	30	90	38
10	nanobasic silica, solvent-free, 90 °C	70	92	11
11	LDH@TRMS@NDBD@Cu$(NO_3)_2$, solvent-free, r.t.	5	97	this work

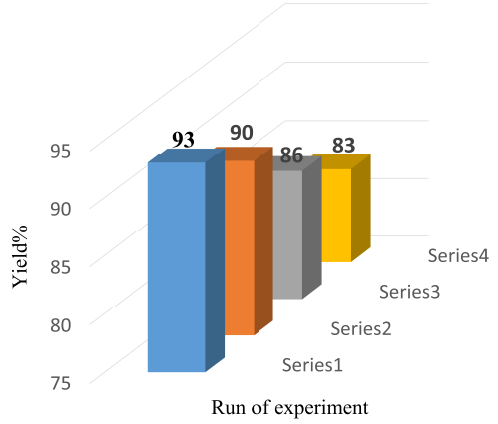

Figure 9. Recyclability of LDH@TRMS@NDBD@Cu in the reaction.

catalyst LDH@TRMS@NDBD@Cu from the reaction mixture through centrifugation. Then, the catalyst was recovered by washing it several times with ethanol and once with acetone before being placed in an oven at 60 °C to dry. According to Figure 9, the catalyst was recycled four times, and no significant decrease in its efficiency was observed. For each run of the model reaction, the catalyst was recovered in the following amounts: first time 0.040 g, second time 0.035 g, third time 0.031 g, and fourth time 0.027 g.

Comparison. To demonstrate the efficiency of the newly synthesized catalyst, a comparison was made with other catalysts in the synthesis of three-component pyranopyrimidine, as shown in Table 4. According to Table 4, the present catalyst significantly improved the reaction conditions. The reaction time was short, and the product yield was high. The reaction was carried out at room temperature, indicating the high efficiency of the new catalyst.

CONCLUSION

Due to the importance of heterocyclic compounds in pharmaceuticals, their preparation method is an important domain of chemistry. Consequently, we endeavored to design a new heterogeneous recyclable nanocatalyst for the one-pot three-component synthesis of pyrano[2,3-*d*]pyrimidine and dihydropyrazolo[4′,3′:5,6]pyrano[2,3-*d*]pyrimidine-dione derivatives. The structure of the new catalyst was checked and verified through different analyses, such as FTIR, EDX, MAPPING, XRD, TGA, DSC, and FESEM. Finally, the efficiency of the catalyst in the one-pot three-component synthesis of pyranopyrimidines was investigated, the reaction was optimized, and the yield was obtained from 88 to 97% in the presence of 0.045 g of the catalyst under solvent-free conditions at room temperature (Table 1). Additionally, dihydropyrazolo[4′,3′:5,6]pyrano[2,3-*d*]pyrimidine-dione derivatives were synthesized through a three-component reaction of 5-methyl-2-phenyl-2,4-dihydro-3*H*-pyrazol-3-one, barbituric acid or 1,3-dimethylbarbituric acid, and aromatic aldehydes, yielding from 88 to 94% in the presence of 0.045 g of catalyst under solvent-free conditions at 45 °C (Table 3). The recyclability of the catalyst was also investigated, demonstrating that the catalyst could be recycled four times without a significant loss of efficiency (Figure 9).

ASSOCIATED CONTENT

Supporting Information

The Supporting Information is available free of charge at https://pubs.acs.org/doi/10.1021/acsomega.3c07913.

Spectral data of synthesized compounds and copies of FTIR, ^{1}HNMR, and^{13}CNMR are shown in the table form (PDF)

AUTHOR INFORMATION

Corresponding Author

Ramin Ghorbani-Vaghei − *Department of Organic Chemistry, Faculty of Chemistry and Petroleum Sciences, Bu-Ali Sina University, Hamedan 65174, Iran*; orcid.org/0000-0001-8322-6299; Email: rgvaghei@yahoo.com, ghorbani@basu.ac.ir

Author

Sarieh Momeni − *Department of Organic Chemistry, Faculty of Chemistry and Petroleum Sciences, Bu-Ali Sina University, Hamedan 65174, Iran*

Complete contact information is available at: https://pubs.acs.org/10.1021/acsomega.3c07913

Author Contributions

S.M. contributed to Laboratory work, preparing data, results analysis, and writing. R.G.-V. is the Supervisor, contributed to result analysis, and presenter of research work. All authors reviewed the manuscript.

Notes

The authors declare no competing financial interest.

https://doi.org/10.1021/acsomega.3c07913
ACS Omega 2024, 9, 10332−10342

■ ACKNOWLEDGMENTS

We thank Bu-Ali Sina University, Center of Excellence Developmental of Environmentally Friendly Methods for Chemical Synthesis (CEDEFMCS) for financial support.

■ REFERENCES

(1) Abdel-Hady, E. E.; Mohamed, H. F. M.; Hafez, S. H. M.; Fahmy, A. M. M.; Magdy, A.; Mohamed, A. S.; Ali, E. O.; Abdelhamed, H. R.; Mahmoud, O. M. Textural Properties and Adsorption Behavior of Zn−Mg−Al Layered Double Hydroxide upon Crystal Violet Dye Removal as a Low Cost, Effective, and Recyclable Adsorbent. *Sci. Rep.* **2023**, *13* (1), 1−19.

(2) Kirar, J. S.; Gupta, N. M.; Chandra, K.; Vani, H. K.; Khare, S.; Tiwari, N.; Deswal, Y. Fabrication and Characterization of Cu Nanoparticles Dispersed on ZnAl-Layered Double Hydroxide Nanocatalysts for the Oxidation of Cyclohexane. *ACS Omega* **2022**, *7* (45), 41058−41068.

(3) Eniola, J. O.; Kumar, R.; Al-Rashdi, A. A.; Ansari, M. O.; Barakat, M. A. Fabrication of Novel Al(OH)3/CuMnAl-Layered Double Hydroxide for Detoxification of Organic Contaminants from Aqueous Solution. *ACS Omega* **2019**, *4* (19), 18268−18278.

(4) Wang, Z.; Zhang, L.; Fang, P.; Wang, L.; Wang, W. Study on Simultaneous Removal of Dye and Heavy Metal Ions by NiAl-Layered Double Hydroxide Films. *ACS Omega* **2020**, *5* (34), 21805−21814.

(5) Boccalon, E.; Viscusi, G.; Sorrentino, A.; Marmottini, F.; Nocchetti, M.; Gorrasi, G. Solvent-Free Synthesis of Halloysite-Layered Double Hydroxide Composites Containing Salicylate as Novel, Active Fillers. *Colloids Surf., A* **2021**, *627*, 127135.

(6) Zheng, H.; Narkhede, N.; Zhang, G.; Zhang, H.; Ma, L.; Yu, S. Highly Dispersed Cu Catalyst Based on the Layer Confinement Effect of Cu/Zn/Ga-LDH for Methanol Synthesis. *Mol. Catal.* **2021**, *516*, 111984.

(7) Wang, H.; Zhou, T.; Li, P.; Cao, Z.; Xi, W.; Zhao, Y.; Ding, Y. Self-Supported Hierarchical Nanostructured NiFe-LDH and Cu3P Weaving Mesh Electrodes for Efficient Water Splitting. *ACS Sustain. Chem. Eng.* **2018**, *6* (1), 380−388.

(8) Rathee, G.; Kohli, S.; Panchal, S.; Singh, N.; Awasthi, A.; Singh, S.; Singh, A.; Hooda, S.; Chandra, R. Fabrication of a Gold-Supported NiAlTi-Layered Double Hydroxide Nanocatalyst for Organic Transformations. *ACS Omega* **2020**, *5* (37), 23967−23974.

(9) Figueiredo, M. P.; Cunha, V. R. R.; Leroux, F.; Taviot-Gueho, C.; Nakamae, M. N.; Kang, Y. R.; Souza, R. B.; Martins, A. M. C. R. P. F.; Koh, I. H. J.; Constantino, V. R. L. Iron-Based Layered Double Hydroxide Implants: Potential Drug Delivery Carriers with Tissue Biointegration Promotion and Blood Microcirculation Preservation. *ACS Omega* **2018**, *3* (12), 18263−18274.

(10) Zhang, P.; Zhu, Y.; Li, Z.; Wang, L.; Yue, C.; Lei, M.; Pu, M. Theoretical Study on Photothermal Properties of Azobenzene Sulfonate/Magnesium-Aluminum Hydroxide Composite Dye. *ACS Omega* **2023**, *8* (12), 11596−11606.

(11) Sheikhan-Shamsabadi, N.; Ghashang, M. Nano-Basic Silica as an Efficient Catalyst for the Multi-Component Preparation of Pyrano[2,3-d]Pyrimidine Derivatives. *Main Gr. Met. Chem.* **2017**, *40* (1−2), 19−25.

(12) Sajjadifar, S.; Gheisarzadeh, Z. Isatin-SO3H Coated on Amino Propyl Modified Magnetic Nanoparticles (Fe3O4@APTES@isatin-SO3H) as a Recyclable Magnetic Nanoparticle for the Simple and Rapid Synthesis of Pyrano[2,3-d] Pyrimidines Derivatives. *Appl. Organomet. Chem.* **2019**, *33* (1), 1−13.

(13) Mohammadi, L.; Heravi, M. M.; Saljooqi, A.; Mohammadi, P. The Preparation of Polyvinyl Imidazole-Functionalized Magnetic Biochar Decorated by Silver Nanoparticles as an Efficient Catalyst for the Synthesis of Spiro-2-Amino-4H-Pyran Compounds. *Sci. Rep.* **2022**, *12* (1), 1−17.

(14) Brahmachari, G.; Nayek, N. Catalyst-Free One-Pot Three-Component Synthesis of Diversely Substituted 5-Aryl-2-Oxo-/Thioxo-2,3-Dihydro-1H-Benzo[6,7]Chromeno[2,3-d]Pyrimidine-4,6,11(5H)-Triones Under Ambient Conditions. *ACS Omega* **2017**, *2* (8), 5025−5035.

(15) Maleki, A.; Niksefat, M.; Rahimi, J.; Taheri-Ledari, R. Multicomponent Synthesis of Pyrano[2,3-d]Pyrimidine Derivatives via a Direct One-Pot Strategy Executed by Novel Designed Copperated Fe3O4@polyvinyl Alcohol Magnetic Nanoparticles. *Mater. Today Chem.* **2019**, *13*, 110−120.

(16) Maddila, S. N.; Maddila, S.; Van Zyl, W. E.; Jonnalagadda, S. B. Mn Doped ZrO2 as a Green, Efficient and Reusable Heterogeneous Catalyst for the Multicomponent Synthesis of Pyrano[2,3-d]-Pyrimidine Derivatives. *RSC Adv.* **2015**, *5* (47), 37360−37366.

(17) Atarod, M.; Safari, J.; Tavakolizadeh, M.; Pourjavadi, A. A Facile Green Synthesis of MgCoFe2O4 Nanomaterials with Robust Catalytic Performance in the Synthesis of Pyrano[2,3-d]-Pyrimidinedione and Their Bis-Derivatives. *Mol. Divers.* **2021**, *25* (4), 2183−2200.

(18) Khurana, J. M.; Vij, K. Nickel Nanoparticles as Semi-heterogeneous Catalyst for One-Pot, Three-Component Synthesis of 2-Amino-4H-Pyrans and Pyran Annulated Heterocyclic Moieties. *Synth. Commun.* **2013**, *43* (17), 2294−2304.

(19) Zolfigol, M. A.; Ayazi-Nasrabadi, R.; Baghery, S. The First Urea-Based Ionic Liquid-Stabilized Magnetic Nanoparticles: An Efficient Catalyst for the Synthesis of Bis(Indolyl)Methanes and Pyrano[2,3-d]Pyrimidinone Derivatives. *Appl. Organomet. Chem.* **2016**, *30* (5), 273−281.

(20) Farahmand, T.; Hashemian, S.; Sheibani, A. Efficient One-Pot Synthesis of Pyrano[2,3-d]Pyrimidinone and Pyrido [2,3-d] Pyrimidine Derivatives by Using of Mn-ZIF-8@ZnTiO3 Nanocatalyst. *J. Mol. Struct.* **2020**, *1206*, 127667.

(21) Ziarani, G. M.; Faramarzi, S.; Asadi, S.; Badiei, A.; Bazl, R.; Amanlou, M. Three-Component Synthesis of Pyrano[2,3-d]-Pyrimidine Dione Derivatives Facilitated by Sulfonic Acid Nanoporous Silica ($SBA\text{-}Pr\text{-}SO_3H$) and Their Docking and Urease Inhibitory Activity. *DARU J. Pharm. Sci.* **2013**, *21* (1), 1−13.

(22) Daraie, M.; Heravi, M. M.; Tamoradi, T. Investigation of Photocatalytic Activity of Anchored Dysprosium and Praseodymium Complexes on CoFe2O4 in Synthesis of Pyrano[2,3-d]Pyrimidine Derivatives. *ChemistrySelect* **2019**, *4* (36), 10742−10747.

(23) Yelwande, A. A.; Lande, M. K. An Efficient One-Pot Three-Component Synthesis of 7-Amino-2, 4-Dioxo-5-Aryl-1,3,4,5-Tetrahydro-2 H-Pyrano[2,3-d]Pyrimidine-6-Carbonitriles Catalyzed by SnO2/SiO2 Nanocomposite. *Res. Chem. Intermed.* **2020**, *46* (12), 5479−5498.

(24) Abdtawfeeq, T. H.; Farhan, Z. A.; Al-Majdi, K.; Jawad, M. A.; Zabibah, R. S.; Riadi, Y.; Hadrawi, S. K.; AL-Alwany, A.; Shams, M. A. Ultrasound-Assisted and One-Pot Synthesis of New Fe3 O4 /Mo-MOF Magnetic Nano Polymer as a Strong Antimicrobial Agent and Efficient Nanocatalyst in the Multicomponent Synthesis of Novel Pyrano[2,3-d]Pyrimidines Derivatives. *J. Inorg. Organomet. Polym. Mater.* **2023**, *33* (2), 472−483.

(25) Khalaj, M.; Mousavi-Safavi, S. M.; Farahani, N.; Lipkowski, J. MgO Nanopowders Catalyzed Synthesis of Pyrano[4,3-d]Thiazolo-[3,2-a]Pyrimidine Derivatives. *Appl. Organomet. Chem.* **2020**, *34* (10), 1−8.

(26) Mamaghani, M.; Hossein Nia, R. A Review on the Recent Multicomponent Synthesis of Pyranopyrazoles. *Polycycl. Aromat. Compd.* **2021**, *41* (2), 223−291.

(27) Tipale, M. R.; Khillare, L. D.; Deshmukh, A. R.; Bhosle, M. R. An Efficient Four Component Domino Synthesis of Pyrazolopyranopyrimidines Using Recyclable Choline Chloride: Urea Deep Eutectic Solvent. *J. Heterocycl. Chem.* **2018**, *55* (3), 716−728.

(28) Heravi, M. M.; Mousavizadeh, F.; Ghobadi, N.; Tajbakhsh, M. A Green and Convenient Protocol for the Synthesis of Novel Pyrazolopyranopyrimidines via a One-Pot, Four-Component Reaction in Water. *Tetrahedron Lett.* **2014**, *55* (6), 1226−1228.

(29) Ziarani, G. M.; Aleali, F.; Lashgari, N.; Badiei, A.; Soorki, A. A. Efficient Synthesis and Antimicrobial Evaluation of Pyrazolopyranopyrimidines in the Presence of SBA-Pr-SO3H as a Nanoporous Acid Catalyst. *Iran. J. Pharm. Res.* **2018**, *172* (2), 525−534.

https://doi.org/10.1021/acsomega.3c07913
ACS Omega 2024, 9, 10332−10342

(30) Sadjadi, S.; Heravi, M. M.; Daraie, M. Heteropolyacid Supported on Amine-Functionalized Halloysite Nano Clay as an Efficient Catalyst for the Synthesis of Pyrazolopyranopyrimidines via Four-Component Domino Reaction. *Res. Chem. Intermed.* **2017**, *43* (4), 2201−2214.
(31) Rigi, F.; Shaterian, H. R. Silica-Supported Ionic Liquids Prompted One-Pot Four-Component Synthesis of Pyrazolopyranopyrimidines, 3-Methyl-4-Aryl-4,5-Dihydro-1H-Pyrano[2,3-c]Pyrazol-6-Ones, and 1,6-Diamino-2-Oxo-1,2,3,4-Tetrahydropyridine-3,5-Dicarbonitriles. *Polycycl. Aromat. Compd.* **2017**, *37* (4), 314−326.
(32) Momeni, S.; Ghorbani-Vaghei, R. Properties, and Application of the New Nanocatalyst of Double Layer Hydroxides in the One-Pot Multicomponent Synthesis of 2-Amino-3-Cyanopyridine Derivatives. *Sci. Rep.* **2023**, *13* (1), 1−12.
(33) Zheng, X.; Wu, K.; Mao, J.; Jiang, X.; Shao, L.; Lin, X.; Li, P.; Shui, M.; Shu, J. Improved Electrochemical Property of Copper Nitrate Hydrate by Multi-Wall Carbon Nanotube. *Electrochim. Acta* **2014**, *147* (3), 765−772.
(34) Beheshti, S.; Safarifard, V.; Morsali, A. Isoreticular Interpenetrated Pillared-Layer Microporous Metal-Organic Framework as a Highly Effective Catalyst for Three-Component Synthesis of Pyrano[2,3-d]Pyrimidines. *Inorg. Chem. Commun.* **2018**, *94*, 80−84.
(35) Mohammadi Ziarani, G.; Hosseini Nasab, N.; Rahimifard, M.; Abolhasani Soorki, A. One-Pot Synthesis of Pyrido[2,3-d]Pyrimidine Derivatives Using Sulfonic Acid Functionalized SBA-15 and the Study on Their Antimicrobial Activities. *J. Saudi Chem. Soc.* **2015**, *19* (6), 676−681.
(36) Saneinezhad, S.; Mohammadi, L.; Zadsirjan, V.; Bamoharram, F. F.; Heravi, M. M. Silver Nanoparticles-Decorated Preyssler Functionalized Cellulose Biocomposite as a Novel and Efficient Catalyst for the Synthesis of 2-Amino-4H-Pyrans and Spirochromenes. *Sci. Rep.* **2020**, *10* (1), 1−26.
(37) Shen, G.; Zhang, L.; Gu, Z.; Zheng, Z.; Liu, Y.; Tan, G.; Jie, X. Zinc Aluminum-Layered Double Hydroxide(LDH)-Graphene Oxide-(GO) Lubricating and Corrosion-Resistant Composite Coating on the Surface of Magnesium Alloy. *Surf. Coat. Technol.* **2022**, *437*, 128354.
(38) Pourkazemi, A.; Asaadi, N.; Farahi, M.; Zarnegaryan, A.; Karami, B. Glucose-Decorated Silica-Molybdate Complex: A Novel Catalyst for Facile Synthesis of Pyrano[2,3-d]-Pyrimidine Derivatives. *Acta Chim. Slov.* **2022**, *69* (1), 30−38.

https://doi.org/10.1021/acsomega.3c07913
ACS Omega 2024, 9, 10332−10342